# Study of Excited Ξ Baryons in $\bar{p}p$-Collisions with the PANDA Detector



2016 J. Phys.: Conf. Ser. 742 012028

(http://iopscience.iop.org/1742-6596/742/1/012028)

Journal of Physics: Conference Series **742** (2016) 012028 doi:10.1088/1742-6596/742/1/012028

# Study of Excited Ξ Baryons in p̄p-Collisions with the P̄ANDA Detector

**Jennifer Pütz[1], Albrecht Gillitzer[1], James Ritman[1], Tobias Stockmanns[1] on behalf of the P̄ANDA Collaboration**

[1] Institut für Kernphysik, Forschungszentrum Jülich, 52425 Jülich, Germany

E-mail: j.puetz@fz-juelich.de

**Abstract.** Understanding the excitation pattern of baryons is indispensable for the understanding of non-perturbative QCD. Up to now only the nucleon excitation spectrum has been subject to systematic experimental studies, while very little is known on excited states of double or triple strange baryons. In studies of antiproton-proton collisions, the $\overline{\mathrm{P}}$ANDA experiment is well-suited for a comprehensive baryon spectroscopy program in the multi-strange and charm sector. In the present study we focus on excited $\Xi^-$ states. For final states containing a $\Xi^-\ \bar{\Xi}^+$ pair, cross sections of the order of $\mu$b are expected, corresponding to production rates of $\sim 10^6$/d at a luminosity $L = 10^{31}\,\mathrm{cm}^{-2}\,\mathrm{s}^{-1}$. Here we present the reconstruction of the reaction $\bar{\mathrm{p}}\mathrm{p} \to \Xi(1820)^-\ \bar{\Xi}^+$ with $\Xi(1820)^- \to \Lambda\ \mathrm{K}^-$ and its charged conjugate channel with the $\overline{\mathrm{P}}$ANDA detector.

## 1. Motivation

In QCD the elementary particles of the strong interaction are quarks and gluons, whereas the minimum quark content of hadrons observable in nature is either three quarks (baryons) or a quark-antiquark pair (mesons). How these composite systems emerge is much less understood. To understand the structure of baryons and mesons it is necessary to study the excitation pattern of these particles. In the spectroscopy of baryons one of the main goals is to answer the following questions: Which degrees of freedom are relevant for the excitation mode of baryons? Can they be described by a three-quark or a quark-diquark structure? How important is the dynamics in baryon-meson systems? There is an intense worldwide effort ongoing to study the nucleon and $\Delta$ excitation spectrum with photo-induced reactions. Much less is known on the excitation spectrum of double and triple strange baryons $\Xi$ and $\Omega$. The study of $\Xi$ baryons will provide independent information on the excitation pattern and allows to verify if the picture deduced from the excited nucleon and $\Delta$ states is correct and has a general validity for baryons in the light quark sector. The $\overline{\mathrm{P}}$ANDA detector will give simultaneous access to the excited states of baryons and anti-baryons in $\bar{\mathrm{p}}\mathrm{p} \to \Xi\bar{\Xi}$ + meson(s). The large cross section for these reactions in the order of $\mu$b allows high statistics data to be collected in reasonable time.

## 2. The P̄ANDA Experiment

$\overline{\mathrm{P}}$ANDA has a wide physics program which, besides baryon and meson spectroscopy, includes studies of QCD dynamics, nucleon structure and electromagnetic processes as well as the study of hadrons in nuclei and hypernuclear physics [1]. The $\overline{\mathrm{P}}$ANDA detector consists of two parts,

the Target Spectrometer which has a cylindrical geometry and is placed around the interaction region and the Forward Spectrometer for the reconstruction of high-energy, forward-boosted particles. The specific design allows the $\overline{\mathrm{P}}$ANDA detector to provide almost $4\pi$ acceptance for both charged and neutral particles.
A property of hyperons is their long life time, and hence long decay length. For the reconstruction of these particles a central tracking system is used. This central tracking system consists of the Micro Vertex Detector (MVD), the Straw Tube Tracker (STT) and the Gas Electron Multiplier (GEM) stations. The MVD is a silicon based high precision vertex detector and the innermost sub-detector enclosing the interaction point. The STT consists of gas filled drift tubes arranged in a cylindrical geometry around the beam axis. The GEM stations are also gas based detectors with planar geometry located directly downstream of the STT, and are thus important to reconstruct the trajectories of particles emitted in the forward direction within the Target Spectrometer. This central tracking system provides a high tracking resolution. In addition, the information from these detectors is combined with other components of $\overline{\mathrm{P}}$ANDA to provide a good particle identification.

## 3. Simulation of $\Xi(1820)^-$

In the following we focus on the channel $\bar{\mathrm{p}}\mathrm{p} \to \Xi(1820)^- \bar{\Xi}^+$ and its charge conjugate. The full decay tree is shown in figure 1.

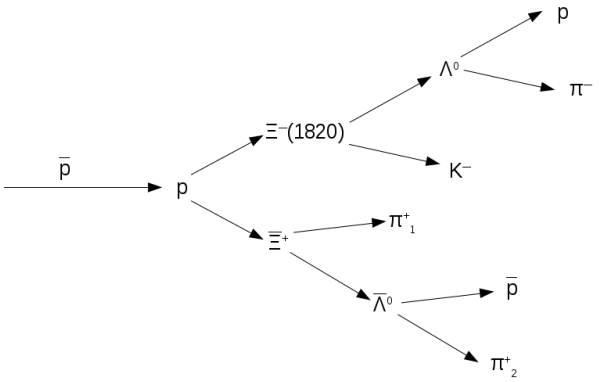


**Figure 1.** Reaction and decay tree for the event generation.

### *3.1. Event Generation*

For this study 1.5 million signal events were generated using the event generator EvtGen [2]. For the charge conjugate channel another 1.5 million events were generated. If not otherwise specified, the charge conjugate process is implicitly included in the following description of the reconstruction strategy. For the production reaction $\bar{\mathrm{p}}\mathrm{p} \to \Xi(1820)^- \bar{\Xi}^+$ the "Phase Space" model, generating an isotropic angular distribution, was used, because a more realistic treatment has not yet been implemented in EvtGen. This simplification does not affect the strategy used in this study. The chosen beam momentum $p_{\bar{p}} = 4.6\,\mathrm{GeV/c}$ corresponds to a center-of-mass energy of 100 MeV above the threshold to produce $\Xi(1820)^-$ and $\bar{\Xi}^+$. The production cross section $\sigma(\bar{\mathrm{p}}\mathrm{p} \to \Xi(1820)^- \bar{\Xi}^+)$ is unknown. However, for the ground state $\Xi^- \bar{\Xi}^+$ production in $\bar{\mathrm{p}}\mathrm{p}$ collisions, a cross section $\sigma \simeq 2\mu\mathrm{b}$ has been measured at $p = 3\,\mathrm{GeV/c}$ [3] and the comparison of ground state and excited single strange hyperon production shows similar cross sections for both species [4]. We therefore assume the cross section $\sigma(\bar{\mathrm{p}}\mathrm{p} \to \Xi(1820)^- \bar{\Xi}^+)$ to be of the order of $1\,\mu\mathrm{b}$. The generated mass distribution for $\Xi(1820)^-$ is shown in figure 2. The properties of $\Xi(1820)^-$

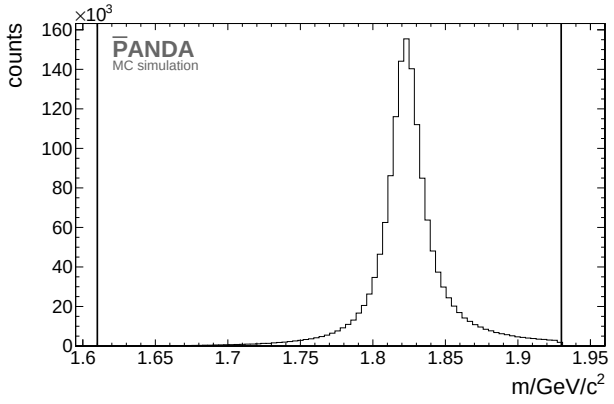


**Figure 2.** Generated mass distribution of $\Xi(1820)^-$. The black vertical lines denote the limits of the kinematically allowed region.

listed below are taken from Ref. [5]. The mass of $\Xi(1820)^-$ is $M = (1.823 \pm 0.005)$ GeV/c$^2$, the width is $\Gamma = (0.024 \pm 0.006)$ GeV/c$^2$. Spin and parity are given as $3/2^-$, however this assignment is still labeled as uncertain.

*3.2. Reconstruction*
For the reconstruction of the $\Xi(1820)^-$ one starts with the final state particles and proceeds backwards through the decay chain.

*3.2.1. Final state particles* The selected final state particles are protons, antiprotons, $\pi^-$, $\pi^+$, $K^-$ and $K^+$ mesons. For the reconstruction of these particles the so-called "ideal pattern recognition" was used. This means that the origin of the hit is extracted from the propagator and all hits are grouped by using this information. The usage of a realistic pattern recognition is foreseen for a more detailed future analysis. To achieve a more realistic reconstruction efficiency, only particles with a minimum number of 4 hits in at least one inner tracking detector (MVD, STT or GEM) are selected. The particle identification (PID) is also "ideal" meaning that the true particle species is selected according to the Monte Carlo (MC) truth value. The reconstruction efficiency for the final state particles is shown in table 1. All reconstruction efficiencies are

**Table 1.** Reconstruction efficiency for $\bar{p}p \to \Xi(1820)^- \bar{\Xi}^+$ (left) and $\bar{p}p \to \bar{\Xi}(1820)^+ \Xi^-$ (right). The error of the efficiency $\sigma_\epsilon \simeq 0.1\%$ is purely statistical.

| final state | $\epsilon$ [%] |
|---|---|
| $\pi^-$ | 83.5 |
| $\pi_1^+$ ($\bar{\Xi}^+$) | 80.9 |
| $\pi_2^+$ ($\bar{\Lambda}$) | 83.1 |
| $K^-$ | 78.6 |
| p | 84.4 |
| $\bar{p}$ | 78.3 |

| final state | $\epsilon$ [%] |
|---|---|
| $\pi^+$ | 83.0 |
| $\pi_1^-$ ($\Xi^-$) | 80.4 |
| $\pi_2^-$ ($\Lambda$) | 82.7 |
| $K^+$ | 83.3 |
| p | 80.7 |
| $\bar{p}$ | 80.9 |

calculated with the MC matched particles and do not include branching ratios in the decay chain.

*3.2.2. Reconstruction of $\Lambda$ and $\bar{\Lambda}$* For the reconstruction of $\Lambda$ hyperons a proton and a $\pi^-$ meson are combined. The same is done with an antiproton and a $\pi^+$ meson for the reconstruction

of $\bar{\Lambda}$ hyperons. After combining the daughter particles, those candidates outside a symmetric invariant mass window around the nominal $\Lambda$ mass of $0.3\,\mathrm{GeV/c^2}$ width are rejected. A kinematic vertex constraint fit is performed on the selected candidate. This means that the tracks of the daughter particles are fitted by taking account of the constraint that the tracks from the daughter particles come from a common vertex point. After the vertex constraint fit, a kinematic mass constraint fit is performed on the fitted candidate. Only those particles which have a probability of $\chi^2$ value larger than 1% in both fits are selected. If more than one candidate fulfilling this condition is found, the candidate with the smallest $\chi^2$ value in the vertex fit is chosen.
For the reconstruction of the $\Lambda$ and $\bar{\Lambda}$ mass, a double-Gaussian fit is performed on the mass distribution of the selected $\Lambda$ and $\bar{\Lambda}$ candidates. The peak position of the inner component of the double-Gaussian fit is taken as the value of the reconstructed mass. Both for $\Lambda$ and $\bar{\Lambda}$ a peak position $M_\Lambda = 1.116\,\mathrm{GeV/c^2}$ in agreement with the input, and a width $\sigma_\Lambda = (2.1 \pm 0.1)\ \mathrm{MeV/c^2}$ is obtained.

*3.2.3. Reconstruction of $\Xi^-$ and $\bar{\Xi}^+$* In contrast to the $\Lambda$ ($\bar{\Lambda}$) decay, the $\Xi^-$ ($\bar{\Xi}^+$) decay contains a neutral particle in the final state. To include this case, an extension of the kinematic vertex fitter was developed. Apart from this, the reconstruction of $\Xi^-$ ($\bar{\Xi}^+$) follows the same procedure as the reconstruction of $\Lambda$ ($\bar{\Lambda}$). For the $\bar{\Xi}^+$ baryon $\bar{\Lambda}$ and $\pi^+$ are combined, for $\Xi^-$ in the charge conjugate channel $\Lambda$ and $\pi^-$. In case of a correct selection for both $\pi^-$ and $\pi^+$ as daughter particle of the $\Lambda$ and $\bar{\Lambda}$, respectively, only one $\pi^-$ or $\pi^+$ candidate remains within the primary particles of the reaction chain, which must be the daughter particle of $\Xi^-$ or $\bar{\Xi}^+$, respectively. The correct selection of $\Lambda$ and $\bar{\Lambda}$ daughter pions is assured by the choice of the best fitted $\Lambda$ and $\bar{\Lambda}$ candidate, as described in the previous section. The pions associated to the $\Lambda$ and $\bar{\Lambda}$ decay are removed from the pion candidate lists used for the reconstruction of $\Xi^-$ and $\bar{\Xi}^+$.
The result of the mass fit for $\bar{\Xi}^+$ reads $M = 1.322\,\mathrm{GeV/c^2}$, $\sigma = (3.69 \pm 0.01)\ \mathrm{MeV/c^2}$ and for $\Xi^-$ reads $M = 1.322\,\mathrm{GeV/c^2}$, $\sigma = (4.00 \pm 0.01)\ \mathrm{MeV/c^2}$.

*3.2.4. Reconstruction of $\Xi(1820)^-$ and $\bar{\Xi}(1820)^+$* In order to reconstruct the excited $\Xi^-$ state, $\Lambda$ and $\mathrm{K}^-$ mesons are combined for $\Xi(1820)^-$ and $\bar{\Lambda}$ and $\mathrm{K}^+$ for $\bar{\Xi}(1820)^+$, using the best candidates of $\Lambda$ and $\bar{\Lambda}$.
The reconstruction scheme is as for $\Xi^-$ and $\bar{\Xi}^+$, but no mass constraint fit is performed. Figure 3 shows the mass distribution of $\Xi(1820)^-$ after different cuts. The resulting mass and width obtained from the double-Gaussian fit are $M_{\Xi^*} = 1.823\,\mathrm{GeV/c^2}$ and $\sigma_{\Xi^*} = (14.2 \pm 0.1)\ \mathrm{MeV/c^2}$ for $\Xi(1820)^-$ and $M_{\bar{\Xi}^*} = 1.823\ \mathrm{GeV/c^2}$ and $\sigma_{\bar{\Xi}^*} = (14.2 \pm 0.1)\ \mathrm{MeV/c^2}$ for $\bar{\Xi}(1820)^+$. The mass values are consistent with the input value.

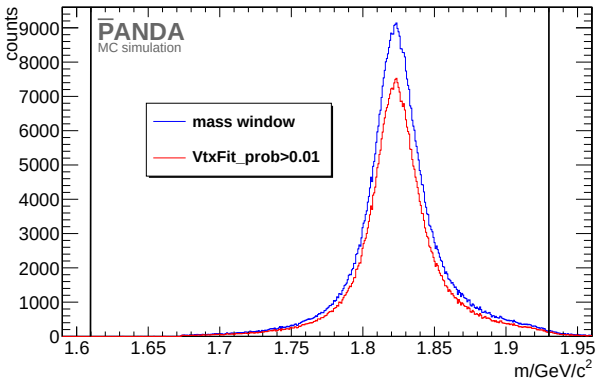


**Figure 3.** Mass distribution for $\Xi(1820)^-$ after the mass cut in blue and after the vertex fit probability cut in red. The black vertical lines denote the limits of the kinematically allowed region.

*3.2.5. Reconstruction of the full decay chain* To reconstruct the full reaction chain $\Xi(1820)^-$ and $\bar{\Xi}^+$ candidates are combined to the initial $\bar{p}p$ system. This is also done with the $\bar{\Xi}(1820)^+$ and $\Xi^-$ for the charge conjugate channel. The resulting four-momentum vector of both daughter particles – here $\Xi(1820)^-$ and $\bar{\Xi}^+$ and their charge conjugate particles – is fitted with the constraint to match to the initial four-momentum vector of the $\bar{p}p$ entrance channel. After the fit only those candidates are selected which have a probability of more than 1 %.

## 4. Background

For background studies 15 million events have been simulated with the Dual Parton Model based generator DPM [6]. Since the ratio of the number of simulated background and signal events does not reflect the ratio of the respective cross section, a scaling factor is needed. The scaling factor $B$ is calculated with the number of generated events and the cross section of signal and background as

$$B = \frac{N_{\mathrm{sig}}^{\mathrm{gen}}/\sigma_{\mathrm{sig}}}{N_{\mathrm{bg}}^{\mathrm{gen}}/\sigma_{\mathrm{bg}}}, \tag{1}$$

where $N_{\mathrm{sig}}^{\mathrm{gen}}$ is the number of generated signal events and $N_{\mathrm{bg}}^{\mathrm{gen}}$ the number of generated background events. The signal and background cross sections are given by $\sigma_{\mathrm{sig}} = 1\,\mu\mathrm{b}$ and $\sigma_{\mathrm{bg}} = 60\,\mathrm{mb}$ [5], respectively. The scaling factor is then $B = 6000$. All background events are subject to the same reconstruction procedure including identical cuts as for the signal events. The number of signal events is 8,614, including the branching ratios: BR($\Lambda \to \pi^-$ p)= 0.639, BR($\Xi^- \to \Lambda\ \pi^-$)= 0.999 and BR($\Xi(1820)^- \to \Lambda\ \mathrm{K}^-$)= 0.3 [5] for the decay tree, but no background events survived the applied cuts.
This means that only a lower limit for the significance can be given as

$$S = \frac{N_{\mathrm{sig}}}{\sqrt{N_{\mathrm{sig}} + N_{\mathrm{bg}} \cdot B}}. \tag{2}$$

In this first study, still based on several simplifications, we would then obtain a significance of 71 for a single background event and a signal-to-background ratio of 1.44:1. To achieve a more realistic estimate of the signal-to-background ratio, the used "ideal" pattern recognition and "ideal" particle identification need to be replaced by realistic ones and the statistical uncertainties must be reduced by generating and analyzing a much larger background sample.

## 5. Summary and Outlook

Each final state particle has a reconstruction efficiency of nearly 80 %. The reconstructed mass for $\Xi(1820)^-$ and $\bar{\Xi}(1820)^+$ are in good agreement with the values in the literature [5]. The topology of the decay chain suppresses the background efficiently. In future studies, the "ideal" particle identification and "ideal" pattern recognition will be replaced by more realistic algorithms. In addition a larger background sample will be generated and analyzed.

## References

[1] Erni W., *et al.* 2009 *arXiv preprint* arXiv: 0903.3905
[2] Lange David J., 2001 *Nucl. Instr. Meth.* A **462**, p. 152
[3] Musgrave B., *et al.* 1965 *Nuovo Cimento* **35**, p. 735
[4] Flaminio V., Moorhead W. G., Morrissson D. R. O. and Rivoire N. 1984 **CERN-HERA84-01**(unpublished)
[5] Olive K. A. *et al.* [Particle Data Group Collaboration] 2014 *Chin. Phys.* C **38** 090001.
[6] Capella A., Sukhatme U., Tan C. I., & Van J. T. T. 1994 *Phys. Rept.* **236** p. 225.